ISSN 1674-1056
http://cpb.iphy.ac.cn
http://iopscience.iop.org/cpb
中国物理 B
Chinese Physics
中国物理 Chinese Physics B

High gain fiber-solid hybrid double-passing end-pumped Nd:YVO_4 picosecond amplifier with high beam quality

Xueyan Dong(董雪岩), Pingxue Li(李平雪), Shun Li(李舜), Dongsheng Wang(王东生)
Citation: Chin. Phys. B . 2020, 29(5): 054207 . **doi:** 10.1088/1674-1056/ab8218
Journal homepage: http://cpb.iphy.ac.cn; http://iopscience.iop.org/cpb

What follows is a list of articles you may be interested in

Noise-like rectangular pulses in a mode-locked double-clad Er:Yb laser with a record pulse energy

Tianyi Wu(吴田宜), Zhiyuan Dou(窦志远), Bin Zhang(张斌), Jing Hou(侯静)
Chin. Phys. B . 2020, 29(1): 014202 . **doi:** 10.1088/1674-1056/ab578a

Self-starting all-fiber PM Er: laser mode locked by a biased nonlinear amplifying loop mirror

Ke Yin(殷科), Yi-Ming Li(李仪茗), Yan-Bin Wang(王彦斌), Xin Zheng(郑鑫), Tian Jiang(江天)
Chin. Phys. B . 2019, 28(12): 124203 . **doi:** 10.1088/1674-1056/ab4d42

$CsPbBr_3$ nanocrystal for mode-locking Tm-doped fiber laser

Yan Zhou(周延), Renli Zhang(张仁栗), Xia Li(李夏), Peiwen Kuan(关珮雯), Dongyu He(贺冬钰), Jingshan Hou(侯京山), Yufeng Liu(刘玉峰), Yongzheng Fang(房永征), Meisong Liao(廖梅松)
Chin. Phys. B . 2019, 28(9): 094203 . **doi:** 10.1088/1674-1056/ab327c

The 2-μm to 6-μm mid-infrared supercontinuum generation in cascaded ZBLAN and As_2Se_3 step-index fibers

Jinmei Yao(姚金妹), Bin Zhang(张斌), Ke Yin(殷科), Jing Hou(侯静)
Chin. Phys. B . 2019, 28(8): 084209 . **doi:** 10.1088/1674-1056/28/8/084209

Pulse generation of erbium-doped fiber laser based on liquid-exfoliated $FePS_3$

Qing Yin(阴晴), Jin Wang(汪进), Xin-Yao Shi(史鑫尧), Tao Wang(王涛), Jie Yang(杨洁), Xin-Xin Zhao(赵新新), Zhen-Jiang Shen(沈振江), Jian Wu(吴坚), Kai Zhang(张凯), Pu Zhou(周朴), Zong-Fu Jiang(姜宗福)
Chin. Phys. B . 2019, 28(8): 084208 . **doi:** 10.1088/1674-1056/28/8/084208

High gain fiber-solid hybrid double-passing end-pumped Nd:YVO_4 picosecond amplifier with high beam quality*

Xueyan Dong(董雪岩), Pingxue Li(李平雪)†, Shun Li(李舜), and Dongsheng Wang(王东生)

Institute of Laser Engineering, Beijing University of Technology, Beijing 100124, *China*

(Received 13 February 2020; revised manuscript received 5 March 2020; accepted manuscript online 23 March 2020)

We propose a fiber-solid hybrid system which consists of a semiconductor saturable absorber mirror (SESAM) mode-locked fiber seed with a pulse width of 10.2 ps and a repetition rate of 18.9 MHz, a two-level fiber pre-amplifier and a double-passing end-pumped Nd:YVO_4 amplifier. In the solid-state amplifier, to enhance the gain and the extraction efficiency, a specially designed structure in which the seed light passes through the gain medium four times and makes full use of population inversion is used as the double-passing amplifier. Besides, the beam filling factor (the ratio of the seed light diameter to the pump light diameter) and the thermal lens effect of the double-passing amplifier are considered and its optical-to-optical conversion efficiency is further improved. To preserve the beam quality of the double-passing amplifier, a new method of spherical-aberration self-compensation based on the principles of geometrical optics is used and discussed. Our system achieves a maximum average power of 9.5 W at the pump power of 28 W, corresponding to an optical-to-optical efficiency of 27%. And the beam quality factor M^2 reaches 1.3 at the maximum output power.

Keywords: picosecond fiber-solid hybrid, double-passing amplifier, high beam quality, spherical-aberration self-compensation

PACS: 42.55.Wd, 42.55.Px, 42.60.Da, 42.55.Xi **DOI:** 10.1088/1674-1056/ab8218

1. Introduction

Picosecond laser at a power of several watts, around a pulse width of ten picoseconds and working at an ultra-high repetition rate (tens of MHz), is widely applied in many fields such as biomedical imaging,[1] surface modification,[2] laser marking,[3] and precision machining.[4] However, in the precise micromachining processing, the processability varies largely with different pulse widths.[5–7] The reason is that all the energy of the pulse with a narrow pulse width (i.e., around ten picoseconds) is transferred to the electrons in a quite short time interval (shorter than the electron-lattice relaxation time). Hence, the nanosecond or longer pulse would lead to melting or evaporation of the lattice due to thermal activation by laser irradiation.[8] Meanwhile, nanosecond pulse width would limit the micro-processing precision, although Q-switch laser machining system has made significant contributions to the industry because of its stable performance.[9] Therefore, it is critical to develop a simple and stable laser source with a pulse width of about 10 ps for promoting the development of laser processing technology.

Many different laser structures can be used for the around ten picosecond pulse lasers. One of these structures is all-fiber laser, which is considered as the most effective way to obtain both high optical-to-optical conversion efficiency and high beam quality.[10,11] But its peak power is restricted by the serious nonlinear effects such as self-phase-modulation (SPM) and stimulated Raman scattering (SRS), etc.[12,13] In order to reduce the nonlinear effects, a highly Yb-doped photonic crystal fiber (PCF) with large mode area and short interaction length has been studied recently.[14] But the high peak power still cannot be obtained due to the nonlinear effect induced by the thin core of optical fiber, especially in the pulse width of shorter than 10 ps regime. In addition, for the air-hole structure of the PCF, serious splicing loss and destruction of the guided wave structure during the fusion-splicing of PCF and conventional optical fiber will cause strong thermal effect and even fatal damage of the fiber. However, the low power all-fiber laser can be used as a seed source and pre-amplifiers for ultrashort pulse laser amplifiers. It can avoid the too long cavity length caused by realizing the multi-longitudinal mode output in the solid locked-mode oscillation and the instability of the oscillation cavity induced by too many spatial light devices. In addition to fiber amplifiers, the solid-state amplifiers are alternative solutions which can reduce the nonlinear effect and sustain high peak power due to the increase of mode area.

Therefore, a fiber-solid hybrid system with a fiber seed source and several solid-state amplifiers has been developed to solve the above defects. In recent years, the domestic and foreign scholars have also conducted research on this scheme. One kind of the hybrid system consists of an all-fiber seed source and a regenerative amplifier,[15,16] which is considered as the most effective way to obtain high gain and high single pulse energy. But it is difficult for this kind of hybrid system to work at thousands of kilohertz repetition, since the length

*Project supported by the National Natural Science Foundation of China (Grant Nos. 61675009 and 61325021) and Key Program of Beijing Municipal Natural Science Foundation, China (Grant No. KZ201910005006).

†Corresponding author. E-mail: pxli@bjut.edu.cn

© 2020 Chinese Physical Society and IOP Publishing Ltd

of the regeneration cavity is limited by the rising edge of the pulse picker. Another kind of hybrid system is the hybrid master oscillator power amplifier (MOPA),[17–19] which is widely used in seed pulse amplification at higher repetition rate. In these configurations, the all-fiber picosecond laser seed source is amplified by the multi-pass amplifier. In the multi-pass amplifier, although the beam filling factor and the thermal effect have been discussed, the extraction efficiency is limited seriously due to the strong thermal lens effect in high power operation. To compensate the positive spherical aberration in gain medium caused by thermal lens effect, aspherical lens[20] or phase conjugate mirrors[21] are used to induce a negative spherical aberration. However, these components are complicated in design due to the high cost in manufacture. Although the method of spherical-aberration compensation has been used to improve the beam quality of multi-pass amplifier in some studies,[22,23] the process of the spherical-aberration self-compensation in four-pass structure based on the principles of geometrical optics has not yet been analyzed in detail. Besides, the partially pumped slab hybrid amplifier has been widely studied,[24] because of the high extraction efficiency and high beam quality. However, there are still a few problems in the slab amplifier such as complex beam shaping for the elongated crystal and large area cooling device. Thus, it is necessary to explore another scheme which combines the simple experimental setup of the multi-pass amplifier with high gain of the slab amplifier.

In this paper, an SESAM mode-locked fiber oscillator with a pulse width of 10.2 ps and a repetition rate of 18.9 MHz is amplified by a two-stage fiber pre-amplifier and a double-passing end-pumped Nd:YVO_4 amplifier. This scheme combines the advantages of fiber laser, such as high beam quality, high electro-optical efficiency and easy access to mode-locked narrow pulse, and those of solid laser, such as being able to reduce the nonlinear effect and sustain high peak power. The output power from the all PM fiber amplifier is 2 W. The laser receives further amplification in the double-passing amplifier and the gain is dramatically enhanced by passing through the gain medium four times. The maximum output power of the double-passing amplifier is 9.5 W at the pump power of 28 W, corresponding to an optical-to-optical efficiency of 27%. The beam quality is well preserved with M^2 factor of 1.3 by the specially designed double-passing structure which is favorable to the spherical-aberration self-compensation. Such a system with narrow pulse width, ultra-high repetition rate, high gain and high beam quality will be valuable for many micromachining processing.

2. Experimental setup

The all PM fiber amplifier includes an SESAM mode-locked fiber oscillator and a two-stage fiber pre-amplifier, as shown in Fig. 1. The oscillator is designed as a linear cavity with a total cavity length of ~ 4.3 m. A single-mode PM Yb-doped fiber is used as a gain fiber and pumped by a single-mode 976 nm laser diode (LD) through a PM wavelength-division-multiplexer (WDM) coupler. An SESAM and a fiber Bragg grating (FBG) are used as the end mirrors of the resonator of the fiber oscillator. A stable mode-locked pulse train at a repetition rate of 18.9 MHz is achieved by using a linear cavity configuration at 50 mW incident pump power, as shown in Fig. 2. When the pump power is 80 mW, 6 mW output power of the oscillator is produced. Figure 3 shows the spectra of the all PM fiber amplifier. The spectrum of the fiber oscillator is centered at 1063.9 nm with a 3-dB spectrum width of 0.3 nm. The spectral ratio of the optical coupler (OC) is 3 : 7. 70% of the oscillating light is injected into the first-stage fiber pre-amplifier, which increases the average power to 60 mW. Meanwhile, the spectrum width is broadened to 0.7 nm due to the self-phase modulation (SPM). To obtain a higher gain, a double-clad Yb-doped gain fiber is used in the second-stage fiber pre-amplifier. Two fiber isolators (ISO) are installed before the two-stage fiber pre-amplifier respectively to isolate the backward laser. A bandpass filter (BPF) with a bandwidth of 2 nm is inserted to reduce the spectrum broadening caused by the SPM. It can be inferred from the Fig. 3 that the central wavelength and 3-dB spectrum width of the second-stage fiber pre-amplifier are respectively 1064.34 nm and 2 nm. There is no cladding light and ASE in the spectra due to the use of cladding light stripper. After the all PM fiber amplifier, the average power is scaled up to 2 W and the near diffraction-limited laser beam is obtained.

The all PM fiber amplifier is followed by the double-passing amplifier. The end-pumped structure is used in the double-passing amplifier because of its low threshold, high conversion efficiency, and high beam quality.[25] The radiation from the all PM fiber amplifier is collimated to a diameter of 2.4 mm before passing through a half-wave plate (HWP1). An isolator (ISO) is used to protect the all PM fiber amplifier against the backward laser from the solid-state amplifier. The 0.6 at.% doped a-cut Nd:YVO_4 as the gain medium has the dimension of $4 \times 4 \times 8$ mm^3, with 2 mm undoped YAG on one side. Because the Nd:YVO_4 crystal shows the best effect at a specific polarization direction, the all PM fiber amplifier is used as a seed of the double-passing amplifier to ensure the linearly polarized input. To dispose the generated thermal load, the Nd:YVO_4 crystal is wrapped by the indium foil and placed in a water-cooled copper heat sink. Both ends of the crystal are respectively coated with 808 nm and 1064 nm anti-reflective coating. The 30 W fiber-coupled semiconductor laser with a 400 μm core diameter and 0.22 NA is used as the pumping source of the double-passing amplifier. The pump light is focused by the coupler 2 with a pump light diameter (D_{pump}) of

400 μm. The accurate position of the pump focus is chosen along the optical axis to maximize the gain. Before being coupled into the double-passing amplifier, the seed light is condensed by the coupler1 which consists of two spherical lenses ($f_{L1} = 225$ mm, $f_{L2} = 30$ mm). The combination of the HWP2 and the Faraday rotator (FR) conserves the horizontally polarized light during the forward pass and rotates it by 90° during the reverse pass. Then the beam passes through a thin-film polarizer (TFP2) and a quarter-wave plate (QWP) successively, and is reflected by a high-reflectivity mirror (HR1). The polarization state of the beam is changed by 90° during the double passes through the QWP. The seed light goes through the Nd:YVO_4 crystal at an incident angle of 8° and is reflected by the flat mirror M3 (HR 1064 nm; HT 808 nm) for the second-passing extraction. Then the single-passing amplified beam is reflected by the HR2 and goes back into the crystal for the third-passing and fourth-passing amplification. The experimental setup of the single-passing amplifier is also shown in Fig. 3. At last, the amplified pulses are outputted by the TFP1. This enables the seed light to pass through the gain medium four times in the double-passing amplifier. The structure makes full use of population inversion and enhances the gain and the extraction efficiency. In comparison with the four-passing amplifier, there is no need to place the quarter wave plate and the polarizer in the cavity, which has the advantages of simple experimental setup and small system cubage.

The spectra of the fiber-solid hybrid amplifier are recorded by a spectrometer (YOKOGAWA, AQ6370D) with a resolution of 0.02 nm. The pulse shapes are monitored by a photodetector (Thorlabs, PDA10CF) which is connected to an oscilloscope (RIGOL, 500 MHz).

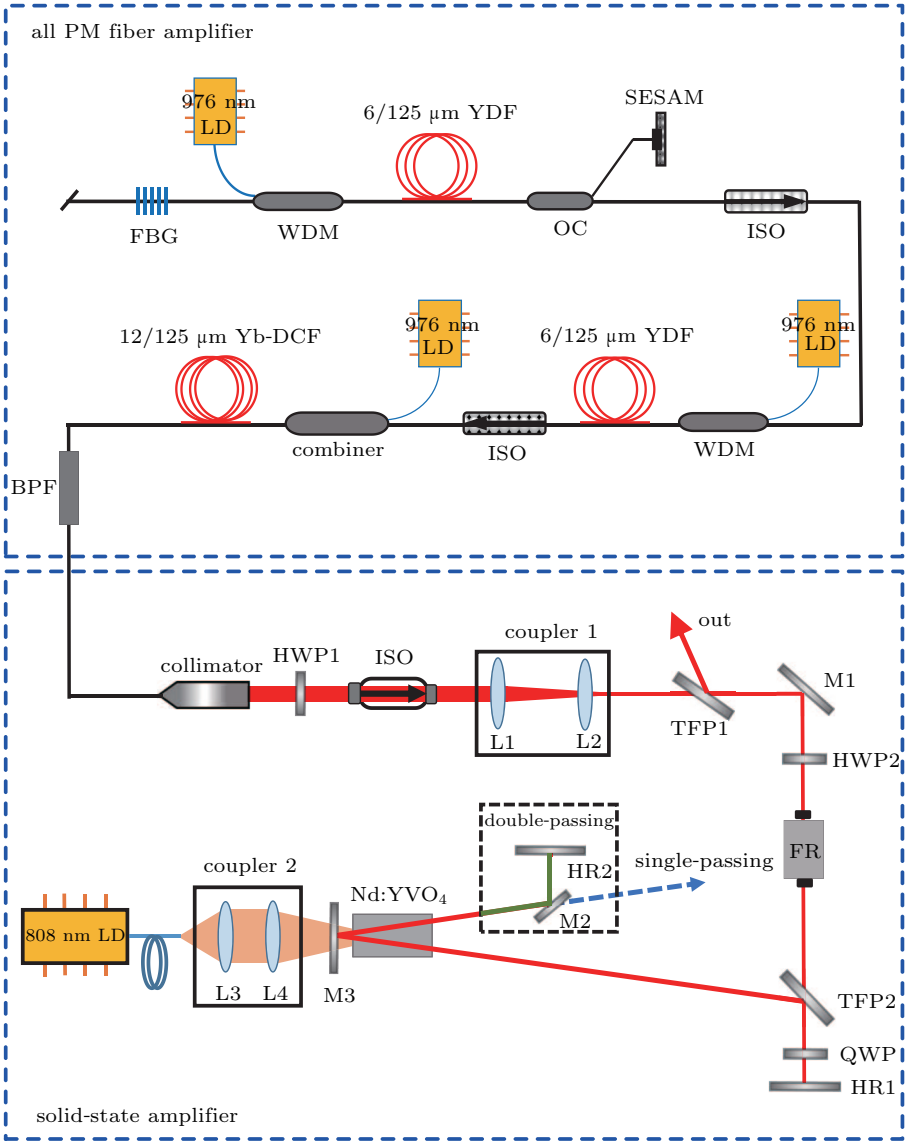


Fig. 1. The schematic layout of the picosecond fiber-solid hybrid amplifier. LD: laser diode; FBG: fiber Bragg grating; OC: optical coupler; SESAM: semiconductor saturable absorber mirror; WDM: wavelength-division-multiplexer; BPF: bandpass filter; YDF: Yb-doped fiber; SMF: single-mode fiber; ISO: isolator; HWP: half-wave plates; FR: Faraday rotator; QWP: quarter-wave plate; HR: high-reflectivity mirror; LD: fiber-coupled laser diode; M: mirror; TFP: thin-film polarizer.

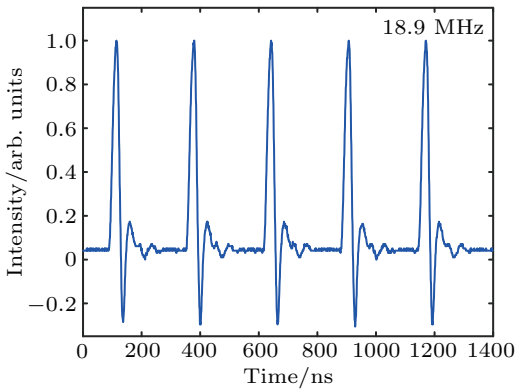


Fig. 2. The mode-locked train of the fiber oscillator.

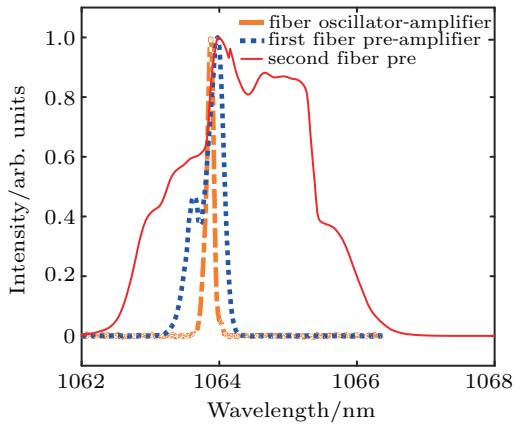


Fig. 3. The spectrum profiles of the all PM fiber amplifier.

3. Experimental results and discussion

3.1. Double-passing power amplification

Firstly, we comparatively analyze the output power and the power gain of the single-passing structure and double-passing structure. Figure 4 shows under the input seed power of 2 W, the average output power is a function of the pump power for both single-passing and double-passing structures. The average output power of 4.2 W is obtained in the single-passing amplification structure with a pump power of 28 W. The average output power of 9.5 W is achieved in the double-passing amplification structure with the same pump power, corresponding to an optical-to-optical efficiency of 27%. And then, we change the input seed power from the all PM fiber amplifier to systematically compare the amplification performance for the two structures with the incident pump power of 28 W. The power gain G is defined as the ratio of the amplified power P_{amp} to the input seed power P_{seed} at 1064 nm. Figure 5 shows that the power gain achieved in the double-passing structure is significantly higher than that of the single-passing structure, especially for the weak seed, and that both of the power gains of the two structures are reduced as the input seed power increases because of the gain saturation effect of the power amplifier.[26] Moreover, the parasitic oscillation effect of the double-passing amplifier in high pump power regime should be studied. In order to suppress the parasitic oscillation, one of the end faces of the crystal is polished to be an oblique angle of 0.5°. Besides, there is an 8° tilt angle between the mirror HR2 and the right end face of the crystal, and a 0.5° tilt angle between the left end face of the crystal and the mirror M3, as shown in Fig. 6. In addition, the higher gain of the double-passing amplifier also helps to suppress the parasitic oscillation effect.

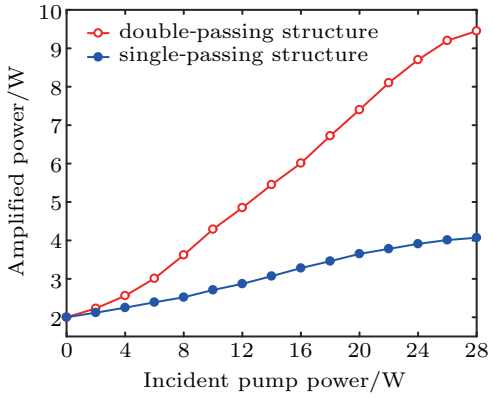


Fig. 4. The output power versus incident pump power for both amplification structures.

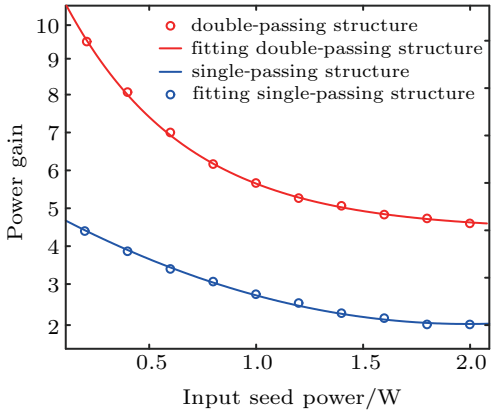


Fig. 5. The power gains as a function of the input seed power.

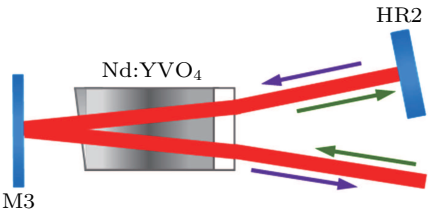


Fig. 6. The laser beam with tilt angle in the four times double-passing amplifier to avoid the parasitic oscillation.

In the double-passing amplifier, since the Nd:YVO_4 crystal damage threshold is 20 kW/cm^2, the pump light diameter should not be less than 350 μm with the maximum pump power of 30 W according to theoretical calculation. The seed light diameters are coupling with the pump light diameters in the double-passing amplifier, the beam filling factor of which is usually chosen to be 0.8 to minimize the deterioration of the

beam quality caused by the thermal effect of the crystal.[27,28] By optimizing the seed light coupler 1 and the pump light coupler 2, we can control the filling factor of the double-passing amplifier. We measure the output powers at the pump light diameters (D_{pump}) of 400 μm, 600 μm, and 800 μm. The results of measurement in Fig. 7 show that the output powers at these diameters are 9.5 W, 5.2 W, and 3.8 W, respectively, and that with the reduction of D_{pump}, the output power increases significantly. To determine the position of the flat mirror HR2, we calculate the thermal focal lengths (f) of the Nd:YVO_4 crystal at different pump diameters. The theoretical value of the thermal focal lengths (f) can be estimated by[29]

$$f = \frac{\pi D_{\text{pump}}^2 K_C}{P_{\text{ph}}(\mathrm{d}n/\mathrm{d}T)}\left[\frac{1}{1-\exp(-\alpha l)}\right], \tag{1}$$

where P_{ph} is the part of pump power that results in waste heat; K_{c} is the thermal conductivity; $\mathrm{d}n/\mathrm{d}T$ is the change rate of refractive index with respect to temperature; α is the crystal absorptivity and l is the crystal length. The parameters P_{ph} =30%, $K_{\text{c}} = 5.23$ W/(K·m), $\alpha = 14.8$ cm^{-1}, $l = 8$ mm, $\mathrm{d}n/\mathrm{d}T = (4.67 \pm 0.6)\times 10^{-6}$ K^{-1} are used. The calculation results are shown in Fig. 8, and it can be seen that the smaller the diameter of the pump light is, the more obvious the thermal lens effect is, and that the thermal focal length is sharply decreased with the increase of the pump light power. The pump light diameter of 400 μm and the seed light diameter of 320 μm are selected respectively. The thermal focal length of the Nd:YVO_4 crystal is 120 mm at the pump power of 28 W. The distance between the flat mirror M3 and the left end face of the crystal is 3 mm, that is to say, the location of the seed light passing through the crystal for the first time is 6 mm away from that of the second time. By using matrix method and ABCD law for Gaussian beam, we compute the equivalent focal length (f') of the single-passing structure and the diameter of the focus light spot. The calculation results of them are 65 mm and 90 μm, respectively. We also calculate the peak power density of laser focused on HR2, which is 0.15 GW/cm^2. This value is much lower than the damage threshold of the film system of high-reflectivity mirror.

During the experiment, we find that the gain bandwidth of the gain medium affects the pulse width due to the gain narrowing effect. In the meantime, the gain matching is important between the central wavelength of the all PM fiber amplifier and the gain spectrum of the double-passing amplifier. The pulse width of the all PM fiber amplifier is 10.2 ps and the spectral width is 2 nm at 1064.34 nm. The central wavelength is 1064.29 nm for Nd:YVO_4 crystal and the gain bandwidth is 0.8 nm. Therefore, the spectral width of the all PM fiber amplifier is about 2.5 times larger than the gain bandwidth of Nd:YVO_4 crystal.

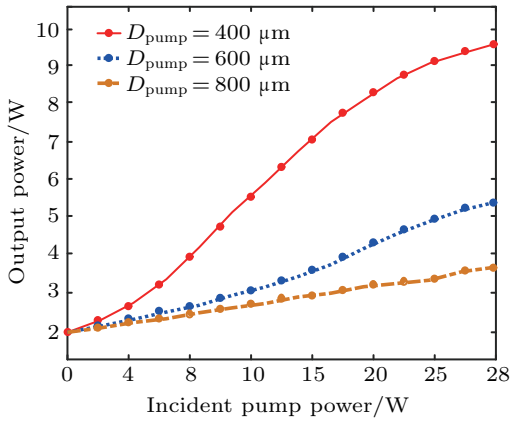


Fig. 7. The output power as a function of pump power with different pump diameters.

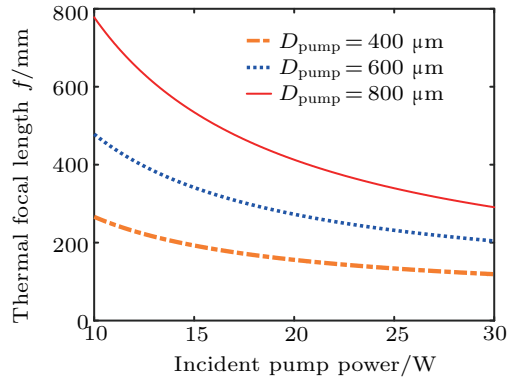


Fig. 8. The focal lengths of the Nd:YVO_4 crystal thermal lens at different pump diameters.

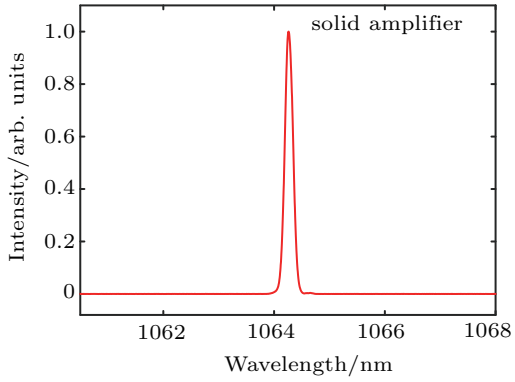


Fig. 9. The output spectrum of the double-passing amplifier.

Figure 9 shows that the spectral width of the double-passing amplifier is narrowed to 0.3 nm, indicating remarkable gain narrowing effect. The temporal intensity profiles of the pulses are also measured by an autocorrelation instrument (APE PulseCheck SM1200), as shown in Fig. 10. It can be seen that the gain narrowing effect broadens the pulse width of the double-passing amplifier to 11.3 ps. Generally, the waveform distortion (the ratio of the amplitude of the pulse front edge to the amplitude of the pulse back edge) is used to measure the temporal profile distortion of the pulse. For the measurement results, there is no waveform distortion caused by the gain saturation in the double-passing amplifier. To test

the output power stability of the fiber-solid hybrid system, we have operated the laser for about 2 hours at the repetition of 18.9 MHz. Figure 11 shows that the instability of the output power is less than 2% in the process of testing.

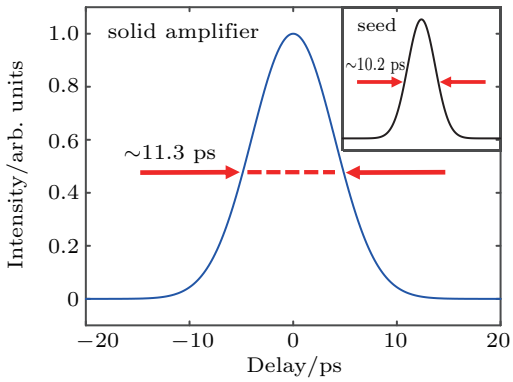


Fig. 10. The temporal intensity profile of the pulse.

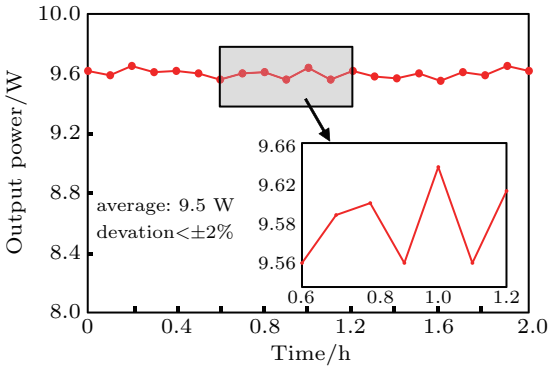


Fig. 11. The power stability of the output beam.

3.2. Beam quality management in double-passing amplifier

Thermal effect always plays an important role in the design of solid-state lasers, especially in high gain configuration. As the pump power of 28 W is tightly concentrated in the small volume of the Nd:YVO_4 crystal, the thermal lens effect is generated significantly. The crystal can be approximately considered as a perfect lens.[30] The spherical aberration caused by the thermal lens will make the focus point discrete and the energy distribution of spot uneven. It is the main reason for the decrease of the output-beam quality in the double-passing amplifier.[31–33] There have been some reports about spherical aberration self-compensation theory in the double-passing structure.[22,23] If the two identical thermal lenses are symmetrically placed about the focus of the laser beam, the degradation of the beam quality caused by the first thermal lens can be compensated by the second thermal lens.

To better understand the phase variation of the beams with positive spherical aberration, we analyze and explain the process according to the principles of geometrical optics. Figure 12(a) demonstrates the distribution of parallel light passing through an ideal lens with negative spherical aberration. Under the effect of negative spherical aberration, the focal length of marginal beam A is shorter than that of paraxial beam B, as shown in Fig. 12(a). The result is that after passing through the focus, the marginal beam A remains to be marginal, and the paraxial beam B remains to be paraxial. Then, the phase difference between the two beams is maintained after passing through the focus. Shown in Fig. 12(b) is the distribution of parallel beam propagating through such a lens. Under the effect of positive spherical aberration, the focal length of marginal beam A is longer than that of paraxial beam B. It can be known from the figure that at some positions behind the focus, the marginal beam might convert into a paraxial beam, and the paraxial beam into a marginal beam. According to the above analysis, the beams with positive spherical aberration may reverse the phase difference signs after passing through a focal point.

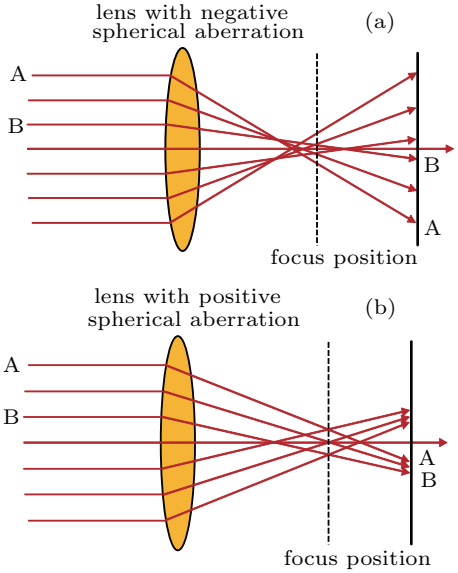


Fig. 12. The distribution of parallel light after passing through lenses. (a) Negative spherical aberration. (b) Positive spherical aberration.

Based on previous theoretical analysis of the spherical aberration compensation, the optical path of the double-passing structure is simulated by the sequence mode of the software ZEMAX (developed by Focus Software Inc.). Since the thermal focal length changes with the pump power, we only simulate the case of the maximum output power. The simulation process is as follows. Firstly, the simulation analysis of the spherical-aberration self-compensation of the single-passing structure is conducted. Then, the spherical aberration is compensated by the double-passing structure. Finally, the aberration analysis results are obtained. In the double-passing amplifier, the first two passes can be equivalent to the first thermal lens with positive spherical aberration, and the last two passes can be equivalent to the second thermal lens, as shown in Fig. 13. According to the calculation results of the equivalent focal length of the single-passing structure in Section 3.1,

the first thermal lens and the second thermal lens can be treated as two identical convex lenses with a focal length of 65 mm. The wavelength of ZEMAX optical system, the entrance pupil diameter, and the field of view are set at 1064 nm, 0.35 μm, and 0°, respectively. The lens data editor is shown in Fig. 14 where the thickness of the convex lens is set at 5 mm and its material is fused quartz. Figure 15 shows the optical pathway diagram of the double-passing structure. We use the Seidel diagram to check the optical aberrations, which can reflect the contribution of each mirror to the system aberration and the overall aberration. As shown in Fig. 16, the Seidel diagram of the single-passing structure shows that the positive spherical aberration is generated when the seed light passes through the second surface (the front surface of the first convex lens) and the third surface (the rear surface of the first convex lens). The equivalent negative spherical aberration is generated when the seed light passes through the fourth surface (the front surface of the second convex lens) and the fifth surface (the rear surface of the second convex lens), as shown in Fig. 17.

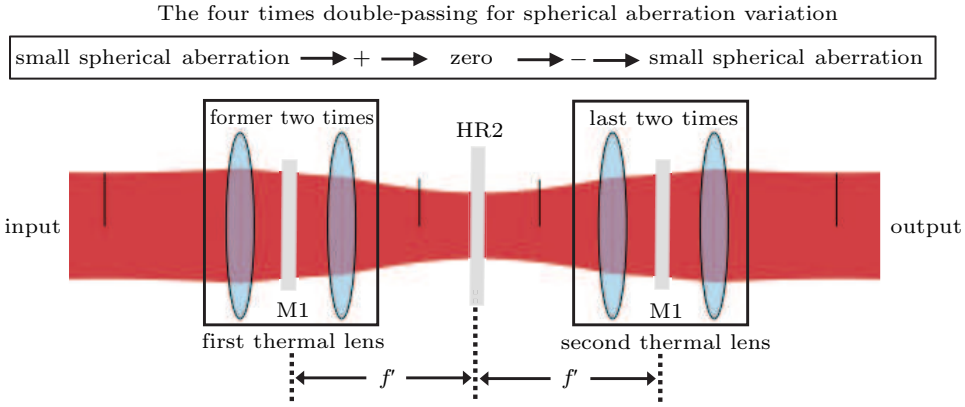


Fig. 13. The sketch of the combined laser amplifier based on spherical aberration compensation theory.

	Surf:Type		Comment	Radius		Thickness		Material		Semi-Diameter	
0	OBJECT	Standard		Infinity		Infinity				0.000	
1	STOP	Standard		Infinity		5.000				2.500	
2	(aper)	Standard	First Thermal Lens	30.000		5.000		F_SILICA		10.000	U
3		Standard		Infinity		62.500				2.371	
4		Standard	Focus Position(HR2)	Infinity		0.000		MIRROR		0.045	
5		Standard		Infinity		62.500				0.032	
6	(aper)	Standard	Second Thermal Lens	Infinity		5.000		F_SILICA		2.371	
7	(aper)	Standard		-30.000	P	0.000				10.000	P
8		Standard		Infinity		5.000				2.500	
9	IMAGE	Standard		Infinity		-				2.500	

Fig. 14. The lens data editor of the double-passing structure.

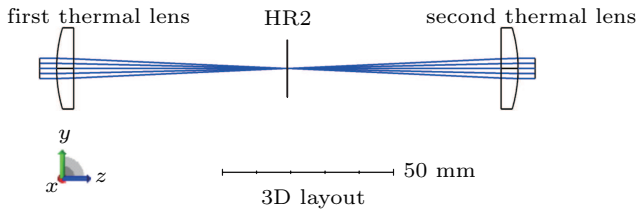


Fig. 15. The optical pathway diagram of the double-passing structure in ZEMAX.

Therefore, on the final image surface, the positive spherical aberration is completely compensated by the negative spherical aberration. At present, many domestic and foreign scholars adopt the theory of spherical aberration compensation in multistage amplifier or traditional double-passing amplifier. In our experiment, the spherical-aberration self-compensation theory is applied to the specially designed structure of double-passing amplifier, which can effectively amplify the fiber seed source while keeping the beam quality constant. Furthermore, based on the principle of geometric optics, we analyze the spherical aberration variation of parallel light after passing through the thermal lens. We also simulate the double-passing amplification process with ZEMAX software, and accurately present the spherical aberration size and the positive and negative correlation. The simulation results show that the spherical aberration of the double-passing amplifier is compensated well and the experimental results are consistent with the simulation results.

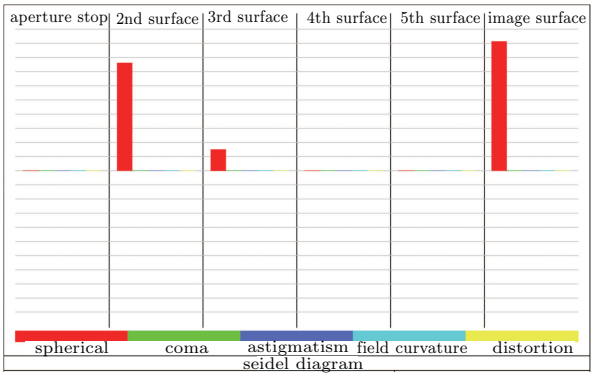


Fig. 16. The Seidel diagram of the single-passing structure.

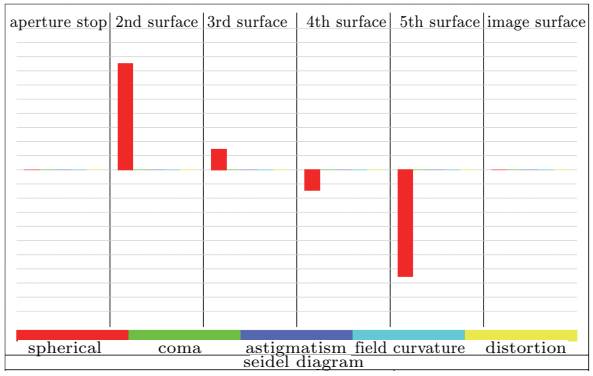


Fig. 17. The Seidel diagram of the double-passing structure.

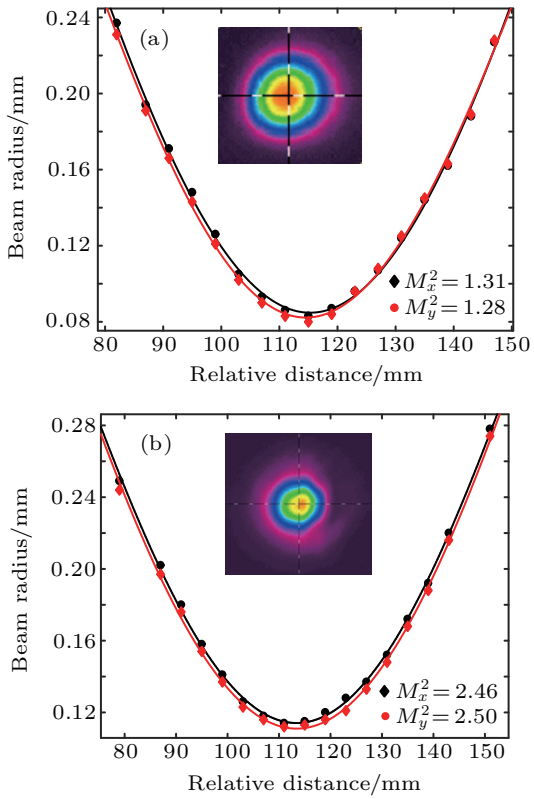


Fig. 18. The beam quality and far-field beam profile with the maximum output power of the (a) double-passing and (b) single-passing structure.

In our experiment, the single-passing amplified beam is focused by the first thermal lens. It is focused on and reflected by HR2. Hence, the position of the flat mirror HR2 is very crucial. The distance between HR2 and the center of the crystal should be adjusted around f' (the equivalent focal length of the single-passing structure) for spherical-aberration self-compensation, as shown in Fig. 13. The beam quality factors M^2 are measured by the 90/10 knife-edge method with Gaussian fitting of the beam radius at several positions for both structures. As shown in Fig. 18(a), the beam quality factors with an average output power of 9.5 W of the double-passing amplification structure are measured to be $M_x^2 = 1.31$ and $M_y^2 = 1.28$, respectively. The far-field distribution (about 4 m from the output end) of the beam is shown in Fig. 18(a) as well. We also measure the beam quality factors and far-field distribution with an average output power of 4.2 W of the single-passing amplification structure shown in Fig. 18(b). The M_x^2 and M_y^2 are 2.46 and 2.50, respectively.

4. Conclusion and perspectives

In our work, we demonstrate a fiber-solid hybrid system based on a two-stage fiber pre-amplifier and a double-passing end-pumped Nd:YVO_4 amplifier with an SESAM mode-locked fiber oscillator as the seed source. In the double-passing amplifier, the seed light from the all-fiber amplifier passes through the gain medium four times to enhance the gain and the extraction efficiency. By optimizing the pump light diameter and the beam filling factor, the optical-to-optical conversion efficiency is further improved. In addition, to improve the beam quality of the double-passing amplifier, the method of spherical-aberration self-compensation base on the principles of geometrical optics is used. The final output laser power reaches 9.5 W with a pulse width of 11.3 ps and a repetition rate of 18.9 MHz. The beam quality is well preserved with M^2 factor of 1.3 at the maximum output power. Compared to the traditional multi-pass amplifier and the slab amplifier, this scheme has the advantages of the higher extraction efficiency and simpler experimental setup. Thus, it is likely to benefit many areas such as material micro-processing, laser ranging, and laser detection.

References

[1] Satata G, Heshmata B, Naika N, Redo-Sanchez A and Raskar R 2016 *Pro. SPIE.* **12** 2222438
[2] Bao J Z, Wang W C, Zhang Y and Zhao Q 2015 *Photon. Res.* **3** 000180
[3] Gedvilas M, Voisiat B and Raciukaitis G 2014 *JLMN* **9** 267
[4] Zhu P, Li J D, Liu Y Q, Chen J, Fu J S, Shi P, Du K and Loosen P 2013 *Opt. Lett.* **38** 004716
[5] Jiang T, Koch J, Unger C, Fadeeva E, Koroleva A, Zhao L Q and Chichkov N B 2012 *Appl. Phys. A* **108** 863
[6] Boerner P, Hajri M, Wahl T, Weixler J and Wegener K J 2019 *J. Appl. Phys.* **125** 234902
[7] Metzner D, Lickschat P and Weissmantel S 2019 *Appl. Phys. A* **125** 411
[8] Ohfuji H, Okuchi T, Odake S, Kagi H, Sumiya H and Irifune T 1993 *Diam. Relat. Mater.* **2** 015
[9] Bai Y, Li H Y, G Shen Z, Song F D, Ren Y Z and Bai T 2009 *Laser Phys. Lett.* **6** 791

[10] Song R, Hou J, Chen S, Yang W and Lu Q 2012 *Appl. Opt.* **51** 2497
[11] Teh P S, Lewis R J, Alam S U and Richardson D J 2013 *Opt. Express* **21** 25883
[12] Tao Y, Xu Z H and Chen S P 2018 *Pro. SPIE.* **12** 2522582
[13] Lin D, Baktash N, Alam U S and Richardson J D 2018 *Opt. Lett.* **43** 004957
[14] Su N, Li P X, Xiao K, Wang X X, Liu J G, Shao Y and Su M 2017 *Chin. Phys. B* **26** 074210
[15] Bai Z A, Fan Z W, Z Bai X, Lian F Q, Kang Z J and Lin W R 2015 *Appl. Sci.* **5** 359
[16] Wang T T, Yu X Y, Zhu B, Li P X and Liu H 2018 *Proc. SPIE* **12** 2522369
[17] Agnesi A, Carra L, Pirzio F, Piccoli R and Reali G 2013 *Opt. Phys.* **30** 2960
[18] Vincent R, Louis D and Yves T 2015 *ASSL* ATh2A.33
[19] Wang D, Wang Y, Liu B, Ye Z B and Liu C 2017 *Pro. SPIE* **12** 2504667
[20] Kasinski J J and Burnham L R 1996 *Appl. Opt.* **35** 5949
[21] Moshe I, Jackel S and Meir A 2007 *Opt. Lett.* **32** 47
[22] Bonnefois M A, Gilbert M, Thro Y P, Weulersse M J 1973 *Opt. Commun.* **08** 041
[23] Wang C H, Liu C, Shen L F, Zhao Z L, Liu B and Jiang H B 2016 *Appl. Opt.* **55** 2399
[24] Chen W, Song Y J, Hu M L, Chai L, Wang C Y, Cui Q J, Guo L, Zhang H L and Liu Q J 2014 *Asia Commun. Photon.* ATh3A.79
[25] Délen X, Balembois F and Georges P 2012 *Opt. Soc. Am. B* **29** 2339
[26] Agnesi A, Carra L, Pirzio F, Piccoli R and Reali G 2012 *Opt. Lett.* **37** 003612
[27] Laporta P and Brussard M 1991 *Quantum Electron.* **27** 2319
[28] Chen Y F, Liao T S, Kao C F, Huang T M, Lin K H and Wang S C 1996 *Quantum Electron.* **32** 2010
[29] Song F, Zhang C B, Ding X, Xu J J, Zhang G Y, Leigh M and Peyghambarian N 2002 *Appl. Phys. Lett.* **81** 2145
[30] Alcock J A, Gendron D J and Nikumb S K 1998 *Pro. SPIE.* **3491**
[31] Hodgson N and Weber H 1993 *Quantum Electron.* **29** 2497
[32] Bourderionnet J, Brignon A, Huignard J P and Frey R 2002 *Opt. Commun.* **204** 299
[33] Liu C, Riesbeck T, Wang X, Ge J, Xiang Z, Chen J and Eichler H J 2008 *Opt. Commun.* **281** 5222